Supporting Information

Enhanced Electrochemical Performance of $NH_4V_4O_{10}$ in Aqueous Zinc-Ion Batteries via PVP Intercalation and Oxygen Vacancy Engineering

Luyao Pan, Yangang Sun*, Song Yao, Yu Zhang, Zhaoxia Wen

College of Chemistry and Chemical Engineering, Shanghai University of Engineering Science, Shanghai 201620, China

E-mail: syg021@sues.edu.cn

Material synthesis

PNVO was prepared by dissolving NH_4VO_3 (0.9524 g) in deionized water (80 mL), followed by adding PVP (0.088 g) and $H_2C_2O_2$ (1.008 g). The mixture was stirred at 60 °C for 30 minutes in a water bath and then subjected to hydrothermal treatment at 180 °C for 24 hours in a 100 mL Teflon-lined autoclave. The resulting product was alternately washed three times with water and ethanol, dried at 80 °C for 12 hours, and subsequently calcined under a nitrogen atmosphere at 300 °C for 2 hours with a heating rate of 5 °C/min to yield PNVO. For comparison, the NVO control sample was prepared using the same procedure but without the addition of PVP and without calcination.

Structure and morphology characterization

The crystal structure of the synthesized materials was analyzed by X-ray diffraction (XRD, Rigaku D/max 2200 PC) using Cu Kα radiation (λ = 1.5406 Å) over a 2θ range of 5° to 90°. Surface chemical composition and electronic states were investigated using X-ray photoelectron spectroscopy (XPS, Thermo Fisher Nexsa). Fourier-transform infrared spectroscopy (FTIR, Thermo Nicolet 6700) was employed to identify chemical bonding and quantify bound water content. Morphological and microstructural features were examined using scanning electron microscopy (SEM, Gemini 300-71-31) and transmission electron microscopy (TEM, JEOL JEM-F200). Thermal stability was evaluated via thermogravimetric and differential scanning

calorimetry (TG-DSC) under a nitrogen atmosphere, with a heating rate of 10 °C/min from room temperature to 500 °C. Additionally, electron paramagnetic resonance (EPR, Bruker A300) was utilized to detect and quantify oxygen vacancies in the materials.

Electrochemical characterization

The cathode materials were prepared by thoroughly mixing the synthesized samples with conductive carbon black and polyvinylidene difluoride (PVDF) binder at a mass ratio of 7:2:1. The mixture was then homogenized with N-methyl-2-pyrrolidone (NMP, 99%) to form a uniform slurry. The resulting slurry was coated onto a titanium current collector and dried in an oven at a predetermined temperature for 12 hours to obtain the final electrode. CR2032 coin cells were assembled using the prepared electrodes, glass fiber separators, and 0.1 mm zinc foils as the anode. Prior to assembly, the zinc foils were polished with sandpaper to remove surface oxides. A 2 mol L^{-1} $ZnSO_4$ aqueous solution (Macklin Corporation) was employed as the electrolyte. **Galvanostatic charge/discharge profiles and galvanostatic intermittent titration technique (GITT) measurements were performed using an automated battery test system (Neware, CT-4008T-5V6A-164). The GITT protocol consisted of 20 min discharging pulses at 0.02 A g^{-1} alternating with 60 min relaxation intervals over 1000 cycles.** Additionally, cyclic voltammetry (CV) and electrochemical impedance spectroscopy (EIS) analyses were performed on a CHI660E electrochemical workstation to evaluate the electrochemical properties of the materials.

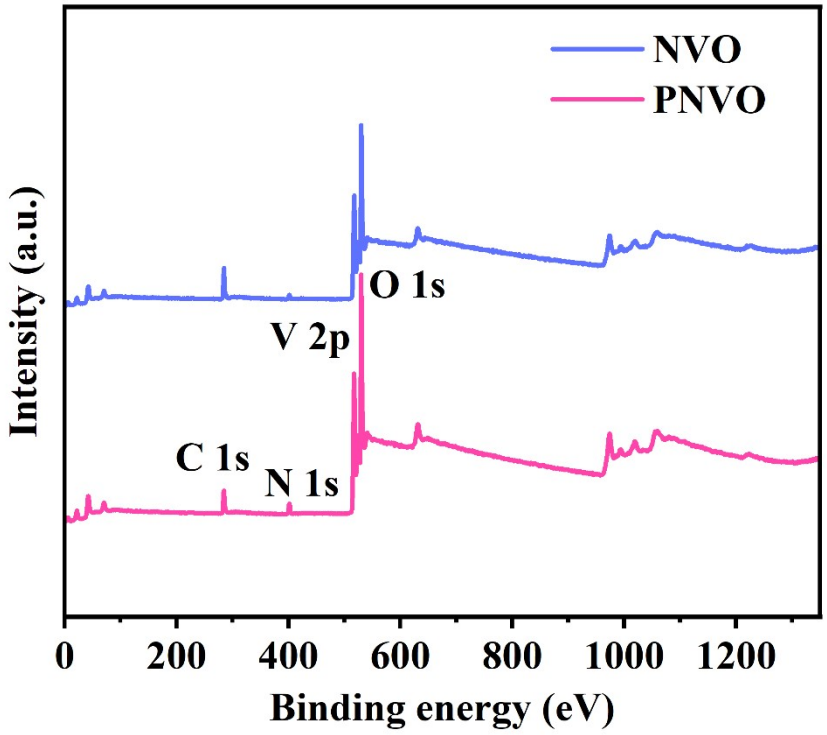

Fig. S1. XPS survey spectrum of PNVO and NVO.

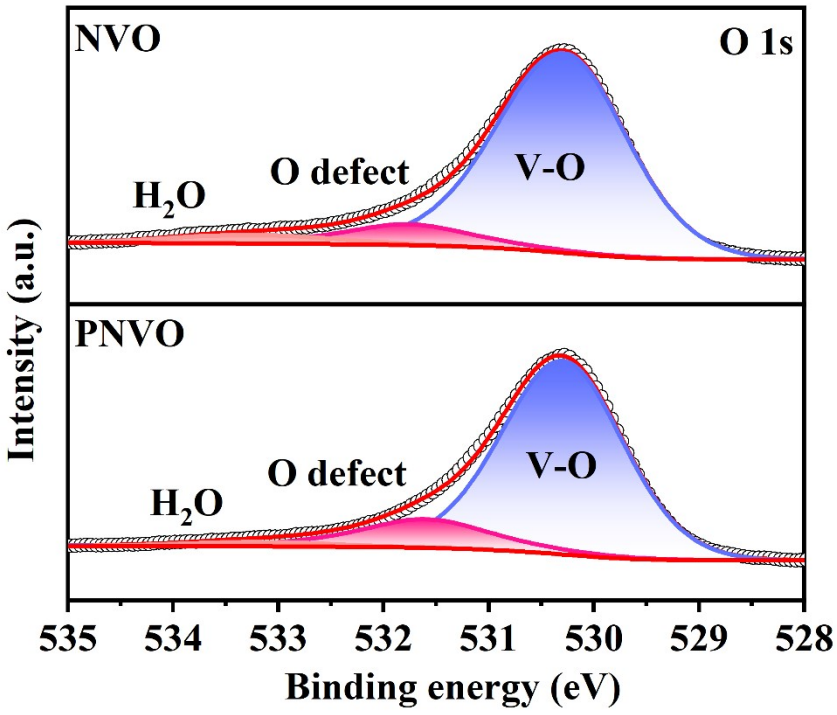

Fig. S2. XPS spectra of O.

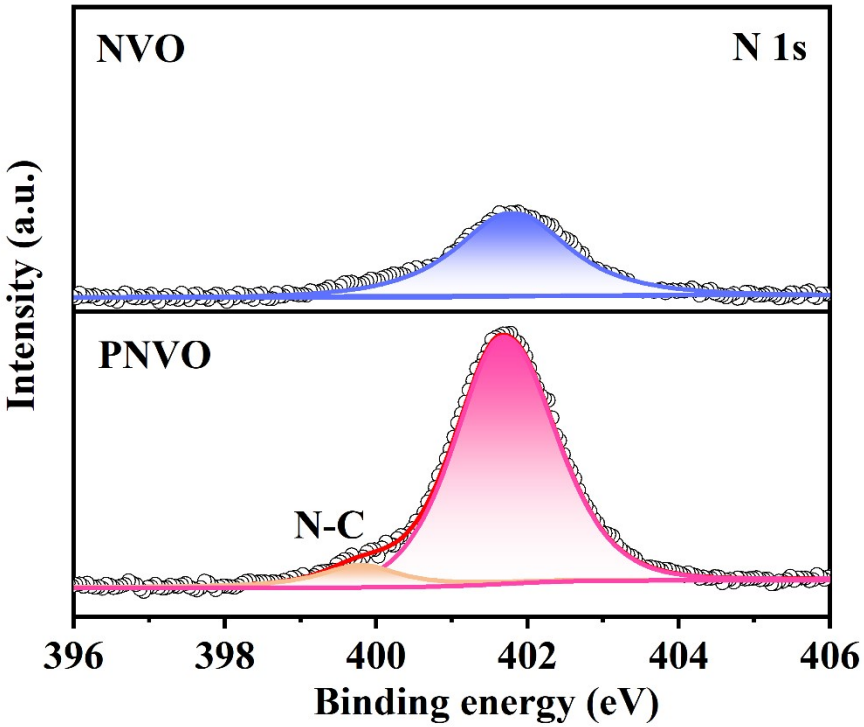

Fig. S3. XPS spectra of N.

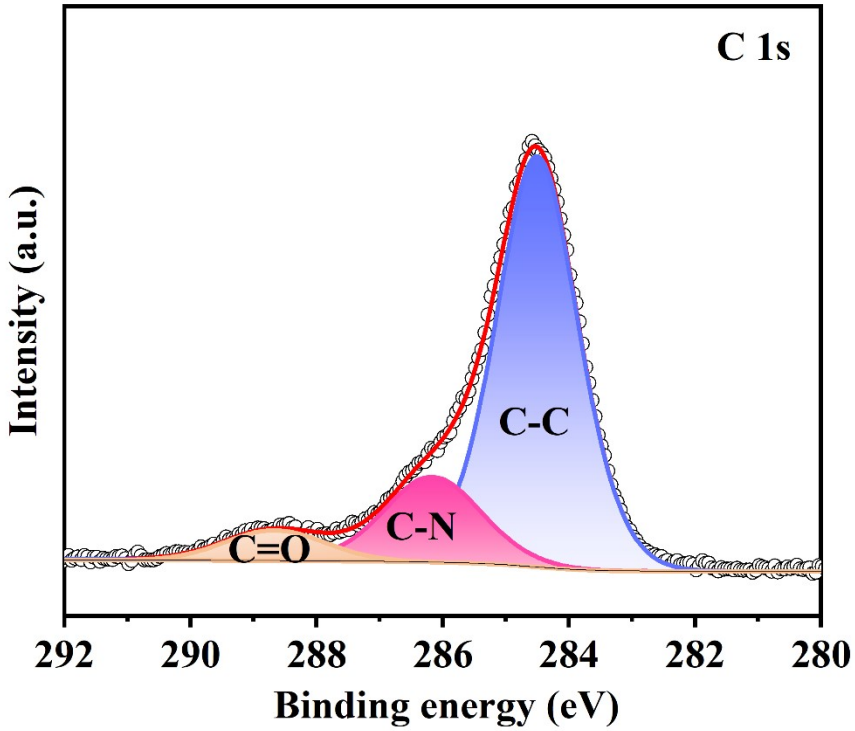

Fig. S4. XPS spectra of C.

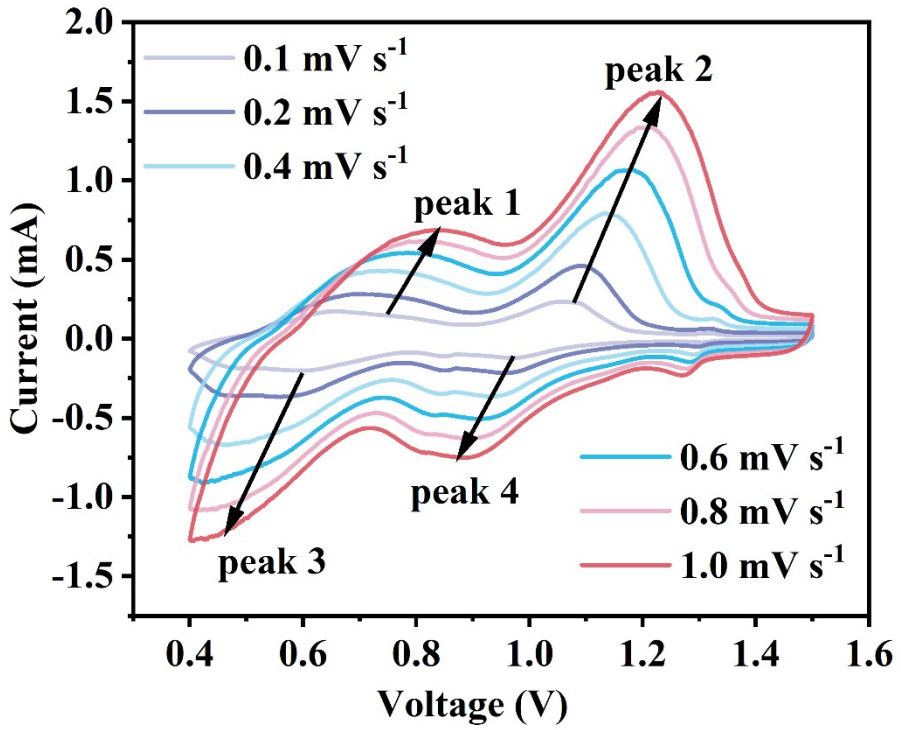

Fig. S5. CV curves of PNVO measured at different scan rates.

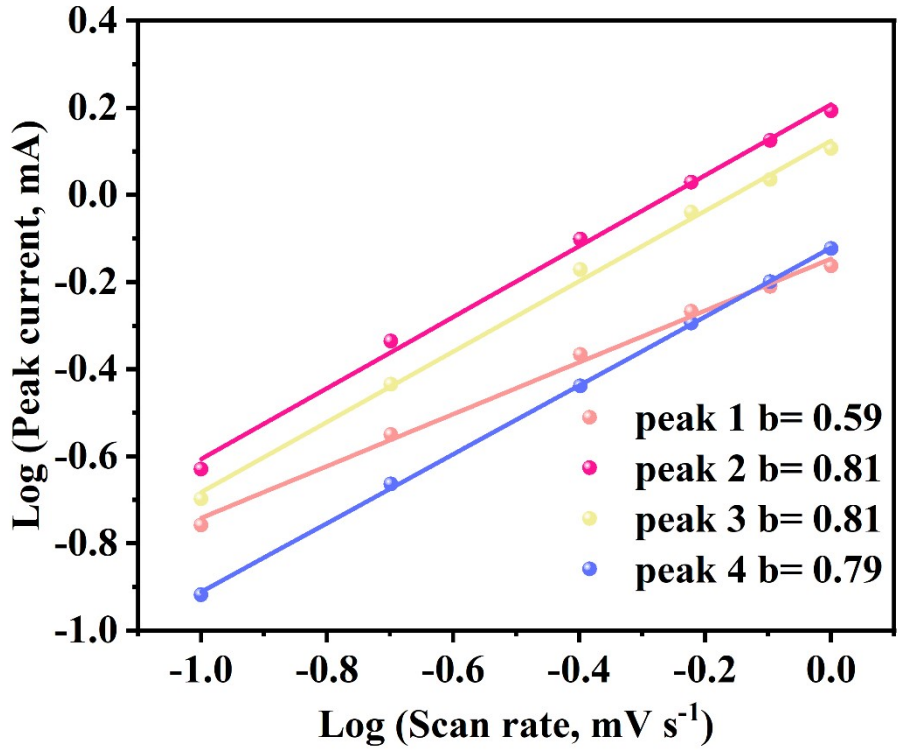

Fig. S6. Corresponding logarithmic plots of peak current (log i) versus scan rate (log v) at specific redox potentials.

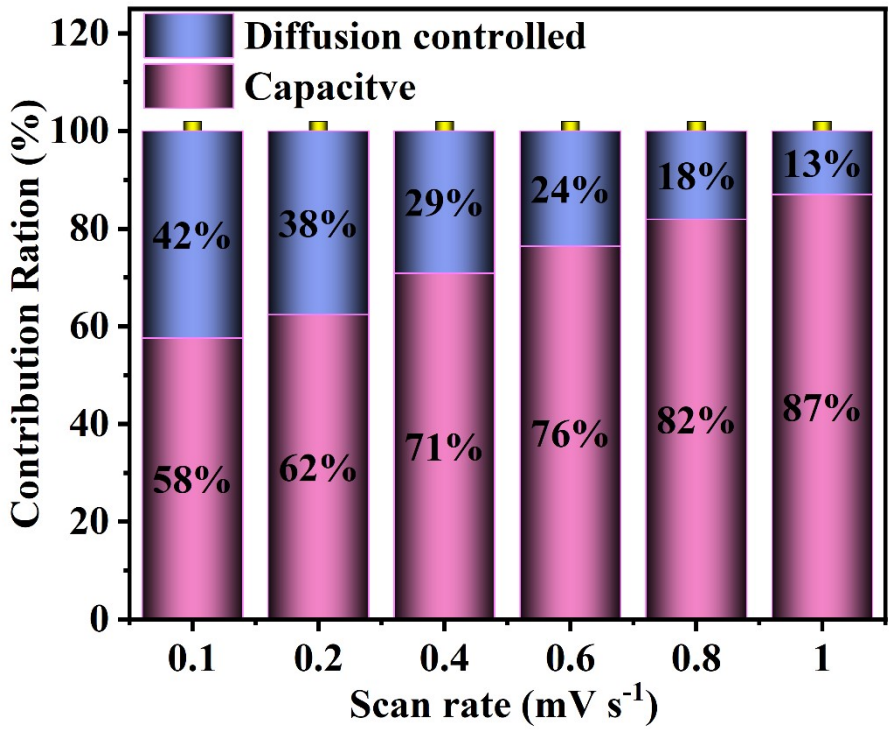

Fig. S7. Quantitative analysis of capacitive and diffusion-controlled contributions to the total charge storage at various scan rates.

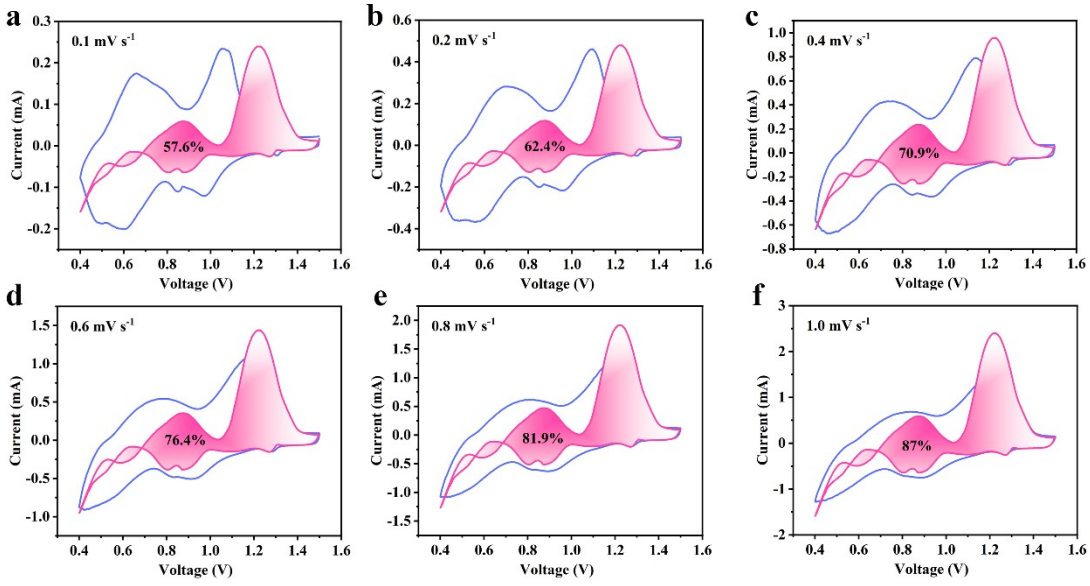

Fig. S8. (a-f) CV curves from 0.1-1 mV s^{-1} of PNVO.

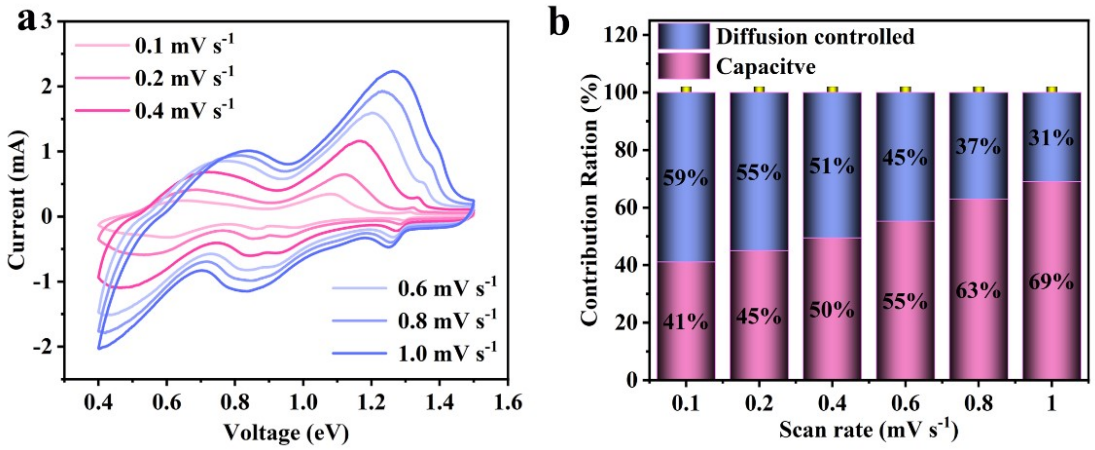

Fig. S9. (a) CV profiles of PNVO at varying scan rates. (c) Capacitive contribution analysis of PNVO at different scan rates.

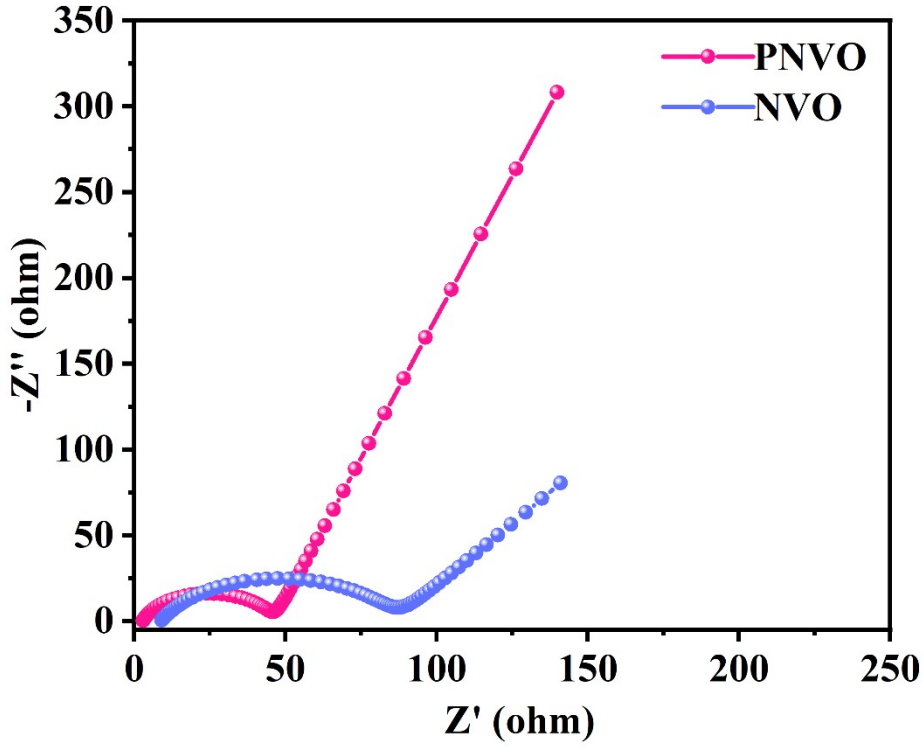

Fig. S10. Nyquist plot

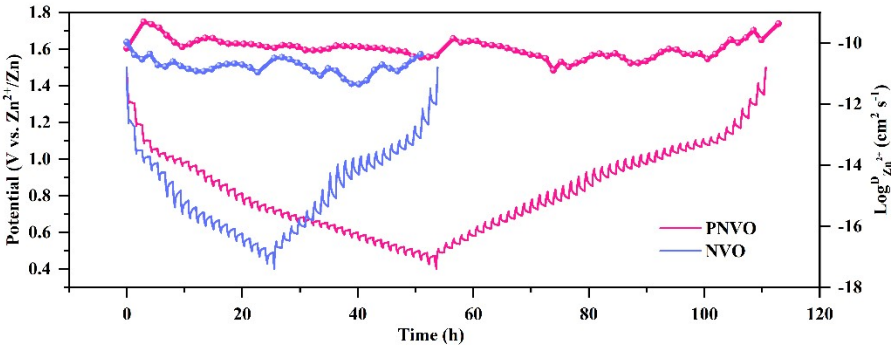

Fig. S11. GITT voltage profiles.